Interleukin-6 inhibition of hERG underlies risk for acquired long QT in cardiac and systemic inflammation

PLOS ONE

RESEARCH ARTICLE

Interleukin-6 inhibition of hERG underlies risk for acquired long QT in cardiac and systemic inflammation

Ademuyiwa S. Aromolaran[1,2], Ujala Srivastava[1,2], Alessandra Alí[3], Mohamed Chahine[4], Deana Lazaro[1], Nabil El-Sherif[1], Pier Leopoldo Capecchi[5], Franco Laghi-Pasini[5], Pietro Enea Lazzerini[5], Mohamed Boutjdir[1,2,6,7]*

1 Cardiovascular Research Program, VA New York Harbor Healthcare System, Brooklyn, New York, United States of America, **2** Department of Cell Biology and Pharmacology, State University of New York Downstate Medical Center, Brooklyn, New York, United States of America, **3** Department of Molecular and Developmental Medicine, University of Siena, Siena, Italy, **4** Centre de Recherche, Institut Universitaire en Santé Mentale de Québec, Department of Medicine, Université Laval, Quebec City, Quebec, Canada, **5** Department of Medical Sciences, Surgery and Neurosciences, University of Siena, Siena, Italy, **6** Departments of Medicine, State University of New York Downstate Medical Center, Brooklyn, New York, United States of America, **7** Department of Medicine, New York University School of Medicine, New York, United States of America

* mboutjdir@gmail.com

Citation: Aromolaran AS, Srivastava U, Alí A, Chahine M, Lazaro D, El-Sherif N, et al. (2018) Interleukin-6 inhibition of hERG underlies risk for acquired long QT in cardiac and systemic inflammation. PLoS ONE 13(12): e0208321. https://doi.org/10.1371/journal.pone.0208321

Editor: Alexander G. Obukhov, Indiana University School of Medicine, UNITED STATES

Received: March 9, 2018

Accepted: November 15, 2018

Published: December 6, 2018

Data Availability Statement: All relevant data are included within the paper itself.

Funding: This work was funded by the American Heart Association (13SDG16850065), http://www.heart.org/HEARTORG/; Merit Review grant I01 BX002137; and Biomedical Laboratory Research & Development Service of Veterans Affairs Office of Research and Development, https://www.research.va.gov/services/blrd/.

Competing interests: The authors have declared that no competing interests exist.

Abstract

Increased proinflammatory interleukin-6 (IL-6) levels are associated with acquired long QT-syndrome (LQTS) in patients with systemic inflammation, leading to higher risks for life-threatening polymorphic ventricular tachycardia such as *Torsades de Pointes*. However, the functional and molecular mechanisms of this association are not known. In most cases of acquired LQTS, the target ion channel is the human ether-á-go-go-related gene (hERG) encoding the rapid component of the delayed rectifier *K* current, I_{Kr}, which plays a critical role in cardiac repolarization. Here, we tested the hypothesis that IL-6 may cause QT prolongation by suppressing I_{Kr}. Electrophysiological and biochemical assays were used to assess the impact of IL-6 on the functional expression of I_{Kr} in HEK293 cells and adult guinea-pig ventricular myocytes (AGPVM). In HEK293 cells, IL-6 alone or in combination with the soluble IL-6 receptor (IL-6R), produced a significant depression of I_{Kr} peak and tail current densities. Block of IL-6R or Janus kinase (JAK) reversed the inhibitory effects of IL-6 on I_{Kr}. In AGPVM, IL-6 prolonged action potential duration (APD) which was further prolonged in the presence of IL-6R. Similar to heterologous cells, IL-6 reduced endogenous guinea pig ERG channel mRNA and protein expression. The data *are first* to demonstrate that IL-6 inhibition of I_{Kr} and the resulting prolongation of APD is mediated via IL-6R and JAK pathway activation and forms the basis for the observed clinical QT interval prolongation. These novel findings may guide the development of targeted anti-arrhythmic therapeutic interventions in patients with LQTS and inflammatory disorders.

Introduction

IL-6 is a pleiotropic cytokine involved in a variety of biological effects including cardiomyocyte response to injury[1]. IL-6 effects occur either through a membrane-bound receptor, the IL-6R α subunit (classical signaling) or a soluble receptor (sIL-6R) [2] complexed with the signal transduction protein glycoprotein 130 (gp130) leading to the activation of the JAK-related signaling pathways [3, 4]. Previous studies demonstrated that circulating IL-6 levels are elevated in patients with autoimmune-inflammatory disorders and may underlie increased vulnerability to QT interval prolongation that contributes prominently to arrhythmic events and Torsade de Pointes (*TdP)* [5–7].

Cardiac and systemic inflammation are associated with the prolongation of corrected QT (QT_c) and higher propensity to develop *TdP*, as demonstrated by accumulating data obtained from patients with myocarditis/endocarditis [8], and systemic autoimmune diseases, particularly rheumatoid arthritis (RA) [9], and other connective tissue disease (CTD) [7], as well as in apparently healthy subjects from the general population [10].

Among systemic autoimmune diseases, the largest evidence involves RA and other CTDs. In RA, a chronic disease with high-grade inflammatory burden, the risk of cardiac arrest and sudden cardiac death (SCD) is ~2 times higher than in non-RA patients [11, 12]. Furthermore, prolonged QT_c is seen in RA patients [13, 14] and has also been associated with disease severity [14, 15], altered levels of inflammatory markers, including IL-6 [6], as well as presenting as an independent predictor of mortality [14, 16, 17]. RA patients treated with the anti-IL-6R blocker tocilizumab, have also been shown to display a rapid and significant QT_c shortening, in addition to decreased levels of C-reactive protein (CRP) and TNF-α [9].

Furthermore, a recent study of a large cohort of RA women demonstrated that inflammation, as assessed by circulating IL-6 levels, correlated more strongly with fatal than non-fatal cardiovascular events [18]. In CTDs patients, a high prevalence of QT_c prolongation (up to ~30%) has been reported [7], with circulating IL-1β levels independently predicting the presence of a prolonged QT_c [19]. Noteworthy, 10 cases of drug-induced *TdP* in systemic lupus erythematosus patients were reported in the literature, and although CRP level was specifically assessed only in two cases, nevertheless it was elevated in both [7]. These observations provide initial clues as to the potential direct electrophysiological effects of IL-6 on ion channels that can alter action potential duration (APD) and QT_c interval.

In the heart, the human ether-á-go-go-related gene, hERG (or KCNH2), which encodes the pore-forming subunit of the rapidly activating component of I_{Kr}, is critical for cardiac repolarization [20, 21]. The functional depression of I_{Kr} by either drugs, genetic defects or inhibiting autoantibodies [22] causes delayed repolarization leading to prolongation of the QT_c on the surface electrocardiogram (ECG) [23] predisposing to SCD [24]. Emerging experimental evidence has shown that inflammatory responses mainly via TNF-α, IL-1β, and IL-6 regulate cardiomyocyte electrophysiological properties [25–29]. TNF-α has been shown to decrease I_{Kr} and the transient outward current (I_{to}) that is also inhibited by IL-1β [30], while IL-1β [28] and IL-6 [31] increase L-type Ca current ($I_{Ca,L}$) altogether leading to prolongation of APD [28]. However, it is unknown whether IL-6 affects cardiac I_{Kr}.

Recently, we showed increased circulating levels of IL-6 in both RA patients and unselected general population with *TdP* [5], with no measurable changes in TNF-α or IL-1. This outcome led us to hypothesize that selective pathological increases in IL-6 may affect hERG/I_{Kr}, thereby contributing to arrhythmias associated with autoimmune-inflammatory responses [8]. Here, we unravel a novel autoimmune/inflammatory channelopathy as a risk factor for SCD whereby IL-6-mediated inhibition of I_{Kr} underlie QT_c prolongation seen in these patients.

Methods

HEK293 cells stably expressing hERG channel

The stably transfected HEK293 cells with hERG channel (HEK-hERG) were a kind gift from Dr Gail Robertson from the University of Wisconsin Madison. They were cultured in Dulbecco's minimum essential medium (DMEM) supplemented with 10% fetal bovine serum and 100 μg/ml geneticin (G418, Gibco; Grand Island, NY, USA). Cells were washed twice with standard DMEM medium and stored in this medium at room temperature for later use. A coverslip with adherent HEK-hERG cells was placed on the glass bottom of a recording chamber (0.8–1 ml in volume) mounted on the stage of an inverted microscope (Diaphot, Nikon). The internal solution contained (in mmol/L): 130 KCl, 1 $MgCl_2$, 0.4 GTP, 5 EGTA, 5 K_2ATP, and 10 HEPES (pH 7.2). External solution contained (in mmol/L): 137 NaCl, 4 KCl, 1.8 $CaCl_2$, 1 $MgCl_2$, 10 Glucose, and 10 HEPES (pH 7.4). When filled with internal solution, the pipette resistance was typically 1.5–2 MOhm. Series resistance was compensated 80–90% before each recording. Membrane potentials were corrected for liquid junctional potential. Population current-voltage (*I–V)* curves were generated by step depolarizations (-60 to +60 mV), from a holding potential of -80 mV in 10 mV increments for 1 s, followed by a repolarizing step to -40 mV for 5 s to obtain tail currents (I_{tail}). The voltage dependence of steady-state activation of I_{Kr} in HEK-hERG cells was measured from tail currents recorded at -40 mV following 4 sec steps to voltages in the range -60 to +60 mV and the data fitted using a Boltzmann function to obtain the midpoint of the steady-state activation curve ($V_{1/2}$). Currents were sampled at 20 kHz and filtered at 5 or 10 kHz. Traces were acquired at a repetition interval of 10 s. Here and elsewhere cells were pre-treated with IL-6 (20 ng/ml) alone or IL-6 (20 ng/ml) + IL-6R (25 ng/ml) for 40 minutes before experimentation [31]. For the dose-response experiments, in addition to 20 ng/ml, doses of 4 ng/ml and 80 ng/ml of IL-6 were studied in the presence of a constant dose of IL-6R of 25ng/ml. IL-6R is used because the soluble form of the IL-6R (sIL-6R) has been found in body fluids such as blood and high levels of sIL-6R have been reported in several chronic inflammatory and autoimmune diseases hence the ability to regulate cells lacking IL-6R [2]. All experiments were performed at room temperature.

Guinea-pig ventricular myocytes

Primary guinea pigs' ventricular cardiac myocytes (used in electrophysiological and biochemical assays) were isolated as previously described [20, 32–34]. Briefly, adult male and female Hartley guinea pigs were deeply anesthetized with isoflurane in accordance with the IACUC approval of this study at the VA New York Harbor Healthcare System and conforming to the NIH guidelines. Hearts were excised, Langendorff perfused with Tyrode solution containing (in mM): 118 NaCl, 4.8 KCl, 1 $CaCl_2$, 10 Glucose, 1.25 $MgSO_4$, 1.25 K_2HPO_4 (pH = 7.4) for 5 minutes. The heart was then perfused with Ca^{2+}-free Tyrode solution for 10 minutes before switching to Ca^{2+}-free Tyrode solution containing Collagenase B (final concentration, 0.6 mg/ml; Boehringer Mannheim, Indianapolis, IN) for an additional 6 minutes. The heart was subsequently perfused with high-K solution containing (in mM): 70 KOH, 50 L-glutamic acid (potassium salt), 40 KCl, 10 Taurine, 2 $MgCl_2$, 10 Glucose, 10 HEPES, 5 EGTA, and 1% albumin (pH 7.4, with KOH) for 5–10 minutes. The digested heart tissue was placed in fresh high-*K* solution, minced into smaller pieces and triturated several times to dissociate the cells. The cell suspension was filtered through a mesh and allowed to settle for 15–20 min. The pellet was resuspended in 10% M199 media and plated on laminin-coated coverslips. Cells were patched 6–8 hours after plating. The external solution used for I_{Kr} and I_{K1} recordings contained (in mM): 145 NaCl, 4.5 KCl, 1 $MgCl_2$, 1.8 $CaCl_2$, 10 HEPES, and 10 glucose (pH 7.4). Ca currents

were blocked by the addition of 5 μM nifedipine in the bath solution and the slow delayed rectifier K current (I_{Ks}) was blocked with 100 μM chromanol. The pipette solutions for recording I_{Kr} and I_{K1} contained (in mM): 140 KCl, 10 HEPES, 11 EGTA, 1 $MgCl_2$, 1 $CaCl_2$, 5 MgATP, and 5 K_2ATP; the pH adjusted to 7.2 with KOH. Currents were recorded in the whole-cell, voltage clamp configuration of the patch-clamp technique using an Axopatch-200B amplifier (Axon Instruments, Inc., Burlingame, CA). I_{Kr} was recorded using a short 200 ms depolarizing pulse from a holding potential (HP) of -50 mV and test pulses were applied at various voltages from -40 to +80 mV in a 10 mV increment before returning to -40 mV for tail current recording. I_{K1} was activated from -80 mV to test potential ranging from -120 mV to +10 mV in 10 mV steps for 200 ms. The external solution for I_{Na} recordings contained (in mM): 20 NaCl, 5 CsCl, 115 tetraethylammonium chloride (TEACl), 1 $MgCl_2$, 10 HEPES, and 10 glucose (pH 7.4, with CsOH). L-type Ca current and T-type Ca current were blocked by $CoCl_2$ (5 mM) and $NiCl_2$ (1 mM), respectively. The internal solution contained (in mM): 140 CsCl, 10 NaCl, 3 $MgCl_2$, 5 EGTA, 10 HEPES, and 2 MgATP (pH 7.2, CsOH). I_{Na} was evoked from -80 mV to test potentials ranging from -70 mV to +20 mV in 10 ms steps for 30 ms. Action potentials were recorded from single ventricular myocytes in current-clamp mode by passing depolarizing currents at subthreshold (1.4 X) intensity. Data were sampled with an A/D converter (Digital 1320A, Axon Instruments) and stored on the hard disk of a computer for subsequent analysis. Currents were sampled at 20 kHz and filtered at 5 or 10 kHz. Traces were acquired at a repetition interval of 10 s.

Biochemical assays

Western blots analysis. Whole cell lysates from HEK293 stably expressing hERG channels and freshly isolated guinea pig cardiomyocytes were used for Western blot analysis. The cells were collected by centrifugation for 5 min at 1,000 g and the pellet was lysed using radioimmunoprecipitation assay (RIPA) buffer (Thermo Fisher Scientific, Walthman, MA) and 10% protease inhibitor cocktail (Sigma, St Louis, MO), incubated on ice for 30 minutes and then centrifuged at 15,000 g for 20 min. The supernatant was collected and the proteins concentration was measured with a Bradford protein assay using EnsSpire 2300 Multimode Plate Reader (PerkinElmer, Waltham, MA). Proteins (50 μg/lane HEK-hERG or 100 μg/lane myocytes) were separated on 4–15% Tris-HCl gel (Bio-Rad Laboratories, Hercules, CA) and electroblotted for 2hr onto polyvinylidene difluoride (PVDF) membrane (Biorad Laboratories, Hercules, CA). Non-specific interactions were blocked using 2.5% non-fat milk (Bio-Rad Laboratories, Hercules, CA), 2.5% BSA (Sigma, St Louis, MO) and 0.1% Tween 20 in Tris-Buffered saline. The membrane was then immunoblotted with anti-K_V11.1/hERG (extracellular) antibody (1:150; Alomone, Jerusalem, Israel) or rabbit anti-GAPDH antibody (1:1000; Sigma,St Louis, MO) overnight at 4˚C. GAPDH expression was used as loading control. The membrane was then probed with anti-rabbit IgG HRP-linked secondary antibody (1:5000; Santa Cruz Biotechnology, Dallas, TX) for 1hr at room temperature and signals were visualized with a chemiluminescence kit (Bio-Rad Laboratories, Hercules, CA). Blots were scanned in a C-Digit blot scanner (LI-COR, Lincoln, NE) at high sensitivity to obtain the image. For quantification of Western blot data, the band intensities of proteins of interest were normalized to their respective GAPDH intensities.

Isolation of RNA, cDNA synthesis and RT-PCR. Total RNA was purified using RNeasy fibrous tissue mini-kit (Qiagen, Hilden, Germany). Qubit 2.0 Fluorometer (Thermo Fisher Scientific, Waltham, MA) was used to quantify RNA and to determine the purity of samples. 1 μg RNA was reverse transcribed using High Capacity cDNA Reverse Transcription kit (Applied Biosystems, Waltham, MA) and qPCR was then carried out on cDNA using TaqMan

Fast Advanced Mastermix (Applied Biosystems, Waltham, MA). Genes coding for $KCNH_2$ ($K_v11.1$) and GAPDH were amplified on Applied Biosystem's 7500 Real-Time PCR system. Taqman Gene Expression Assay primers were used, and these were obtained from IDT (Integrated DNA Technologies, Coralville, IA). Primers contained the double quenched probe (5′FAM/ZEN/3′IBFQ) and ROX passive reference dye was used. Gene expression in treated guinea pig cardiomyocytes was represented as a fold change relative to expression in untreated cells.

Data and statistical analyses. Electrophysiological data were analyzed off-line using built in functions in clampfit (pCLAMP 10), and Origin software. Quantification of Western blot data was performed by analyzing band intensities of proteins and then normalized to their respective GAPDH intensities. For all electrophysiology and biochemistry assays, the effect of IL-6 alone or IL-6+IL-6R basal I_{Kr} or hERG expression (mRNA and protein expression) were compared using one-way ANOVA with Bonferroni post-hoc analysis or two-tailed unpaired *t* test for comparisons between groups and considered significant at $P < 0.05$. Data are reported as means ± S.E.M.

Results

IL-6 inhibits I_{Kr} in HEK293 cells

First, we assessed the effects of IL-6 on I_{Kr} current in HEK-hERG cells using the whole-cell patch clamp technique and the protocol shown in *Fig 1A*. Cells were exposed to IL-6 (20 ng/ml) alone or IL-6 (20ng/ml)+IL-6R (25 ng/ml) at concentrations previously shown to modulate $I_{Ca,L}$ in myocytes after 40 minutes pre-incubation [31]. Compared to basal I_{Kr} (*Fig 1B*), cells pre-incubated with IL-6 alone (*Fig 1C*) displayed depressed I_{Kr} densities (*Fig 1E & 1F*). At +20 mV, I_{Kr} peak densities were inhibited by 29.6% (from 44.9±4.43 pA/pF, n = 21, to 31.6 ±2.04 pA/pF, n = 18, $^*P<0.05$, *Fig 1E*), and I_{Kr} tail densities were inhibited by 41.9% at +20 mV (from 66±7.11 pA/pF, n = 21, to 38.3±4.38 pA/pF, n = 18, $^*P<0.05$, *Fig 1F*). In the presence of IL-6R (*Fig 1D*), IL-6 inhibited I_{Kr} peak densities by 53.6% at +20 mV (from 44.9±4.43 pA/pF, n = 21, to 20.8±2.50 pA/pF, n = 9, $^*P<0.05$, *Fig 1E*) and I_{Kr} tail densities by 59.5% at +20 mV (from 66±7.11 pA/pF, n = 21, to 26.7±3.94 pA/pF, n = 9, $^*P<0.05$, *Fig 1F*).

Furthermore, we investigated whether the effect of IL-6 on I_{Kr} is concentration-dependent. At a fixed concentration of IL-6R (25 ng/ml), we assessed the effects of IL-6 at 4 ng/ml and 80 ng/ml of IL-6 on I_{Kr} (*Fig 1G*). At +20 mV, 4 ng/ml of IL-6 reduced I_{Kr} peak densities by 21.9% (from 44.9±4.43 pA/pF to 35.08±5.71 pA/pF, n = 5, $P>0.05$, *Fig 1G*) and reduced I_{Kr} tail densities by 27.2% (from 66±7.11 pA/pF to 48.04±3.52 pA/pF, n = 5, $^*P<0.05$, *Fig 1G*). Increasing IL-6 concentration to 80 ng/ml had a more pronounced effect such that at +20 mV, I_{Kr} peak densities were reduced by 65.3% (from 44.9±4.43 pA/pF to 15.Y±1.74 pA/pF, n = 13, $^*P<0.05$, *Fig 1G*) and I_{Kr} tail densities were reduced by 72.8% (from 66±7.11 pA/pF, to 17.93±2.43 pA/pF, n = 13, $^*P<0.05$, *Fig 1G*). Taken together our data demonstrate that IL-6 inhibition of I_{Kr} is concentration dependent.

We next examined the effect of IL-6 and IL-6+IL-6R on the biophysical properties of I_{Kr}. First, we analyzed and compared the *I-V* relationships for activation measured during the depolarizing steps. I_{Kr} tail currents were normalized to the maximum current at +60 mV and plotted as a function of voltage (mV) and fitted to a Boltzmann equation to obtain activation curves (*Fig 2A*). IL-6 alone (*Fig 2A*), produced a small leftward shift in the midpoint of the steady-state activation (or $V_{1/2}$) from -5.86±2.45 mV (n = 21) to -10.75±1.32 mV (n = 18, $P>0.05$), but produced a significant shift to -14.6±2.11 mV (n = 9, $^*P<0.05$, *Fig 2A*), in the presence of IL-6+IL-6R (*Fig 2A*) respectively.

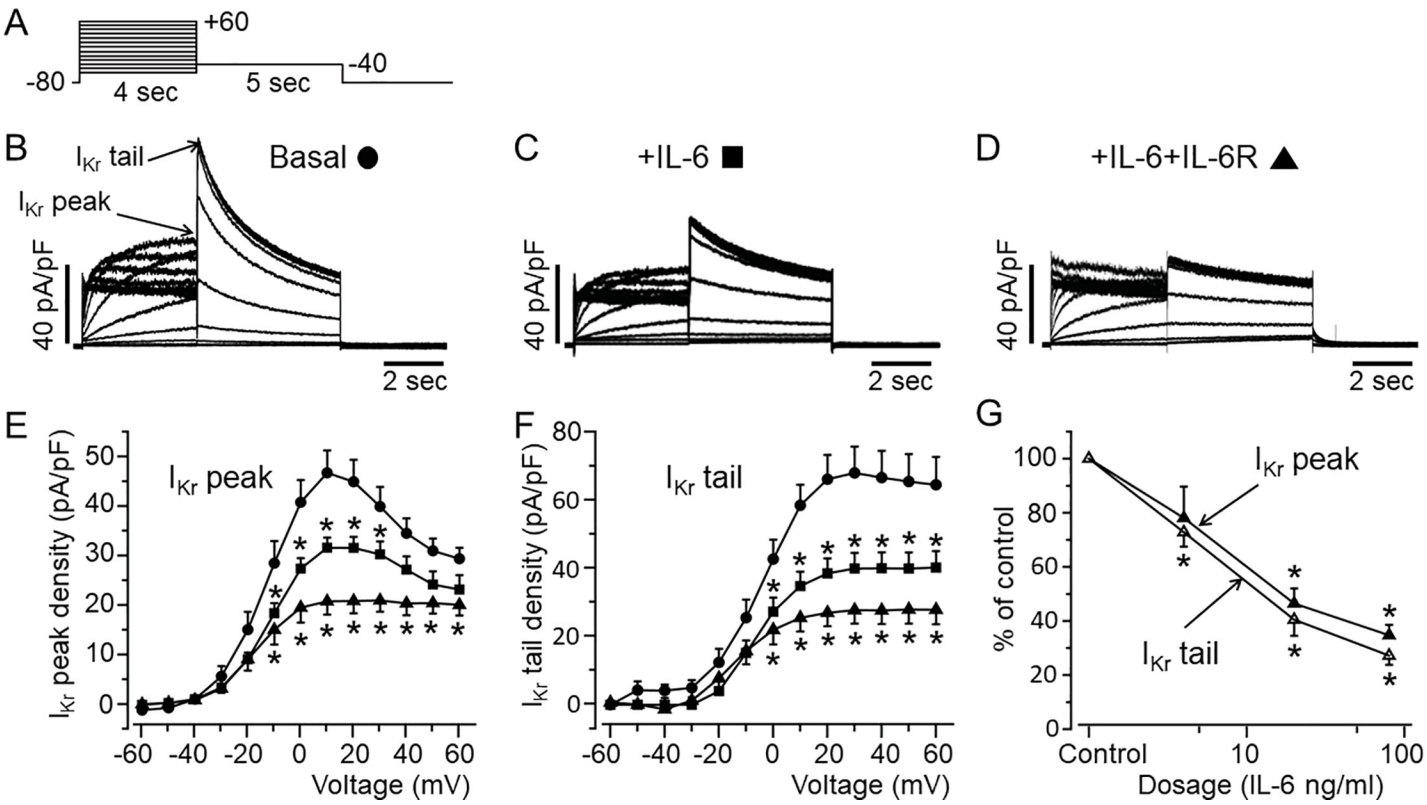

Fig 1. Functional effect of IL-6 on I_{Kr} in HEK-hERG cells. *A*, Voltage-clamp protocol used to elicit I_{Kr} in HEK-hERG cells stable expressing hERG channel. *B*, Control hERG current. *Arrows* indicate hERG peak and tail currents. *C*, I_{Kr} currents measured in cells pre-treated with IL-6 alone or *D*, with IL-6+IL-6R. *E*, I_{Kr} peak and *F*, tail density-voltage- curves for control (circle, n = 21), IL-6 alone (square, n = 18) and IL-6+IL-6R (triangle, n = 9). *G*, The dose-response effects of IL-6+IL-6R on I_{Kr} peak and tail densities. Data were normalized to control and expressed as percentage of control.

https://doi.org/10.1371/journal.pone.0208321.g001

To determine the I_{Kr} activation time course ($\tau_{activation}$), the data were fitted with a single exponential function. I_{Kr} measured in HEK-hERG cells pretreated with IL-6 alone or IL-6+IL-6R produced faster activation kinetics (*Fig 2B*). At +20 mV, $\tau_{activation}$ accelerated from 329±52 ms (n = 21) to 219±16 ms, (n = 18, $^{*}P<0.05$) with IL-6 and to 103.2±20.1 ms (n = 9, $^{*}P<0.05$) in the presence of IL-6+IL-6R demonstrating that IL-6+IL-6R exert a profound effect on the activation kinetics of I_{Kr}. The next series of experiments examined the effects of IL-6 on the inactivation kinetics of I_{Kr}. A three-step protocol (*Fig 2C*) to isolate inactivating currents and determine the kinetics of inactivation was used [35–37]. hERG channels were activated by a 200 ms depolarizing step to +40 mV followed by a brief hyperpolarizing step to -120 mV for 10 ms to allow the channels to recover from inactivation. The hyperpolarizing step was followed by a step to various test potential from -40 mV to +60 mV. The estimated time constant of inactivation ($\tau_{inactivation}$) was measured by fitting the current traces to a single exponential. As illustrated in *Fig 2*, there was no significant difference in current traces and $\tau_{inactivation}$ values obtained for basal I_{Kr} (*Fig 2D*), and currents measured in the presence of IL-6 alone (*Fig 2E*), or IL-6+IL-6R (*Fig 2F*) within the voltage range studied (*Fig 2G*).

Next, we assessed whether IL-6 affected hERG expression in HEK-hERG cells. Western blot analysis was used to examine protein expression of hERG channels in control untreated cells and in cells pretreated for 40 minutes with IL-6 alone or IL-6+ILR. As illustrated in *Fig 3A*, (*Lane 1*), untreated control cells displayed bands at 150 kDa and 135 kDa, which are specific for the hERG channel. Cells pretreated with IL-6 (*Fig 3A*, *Lane 2*), or IL-6+IL-6R (*Fig 3A*, *Lane*

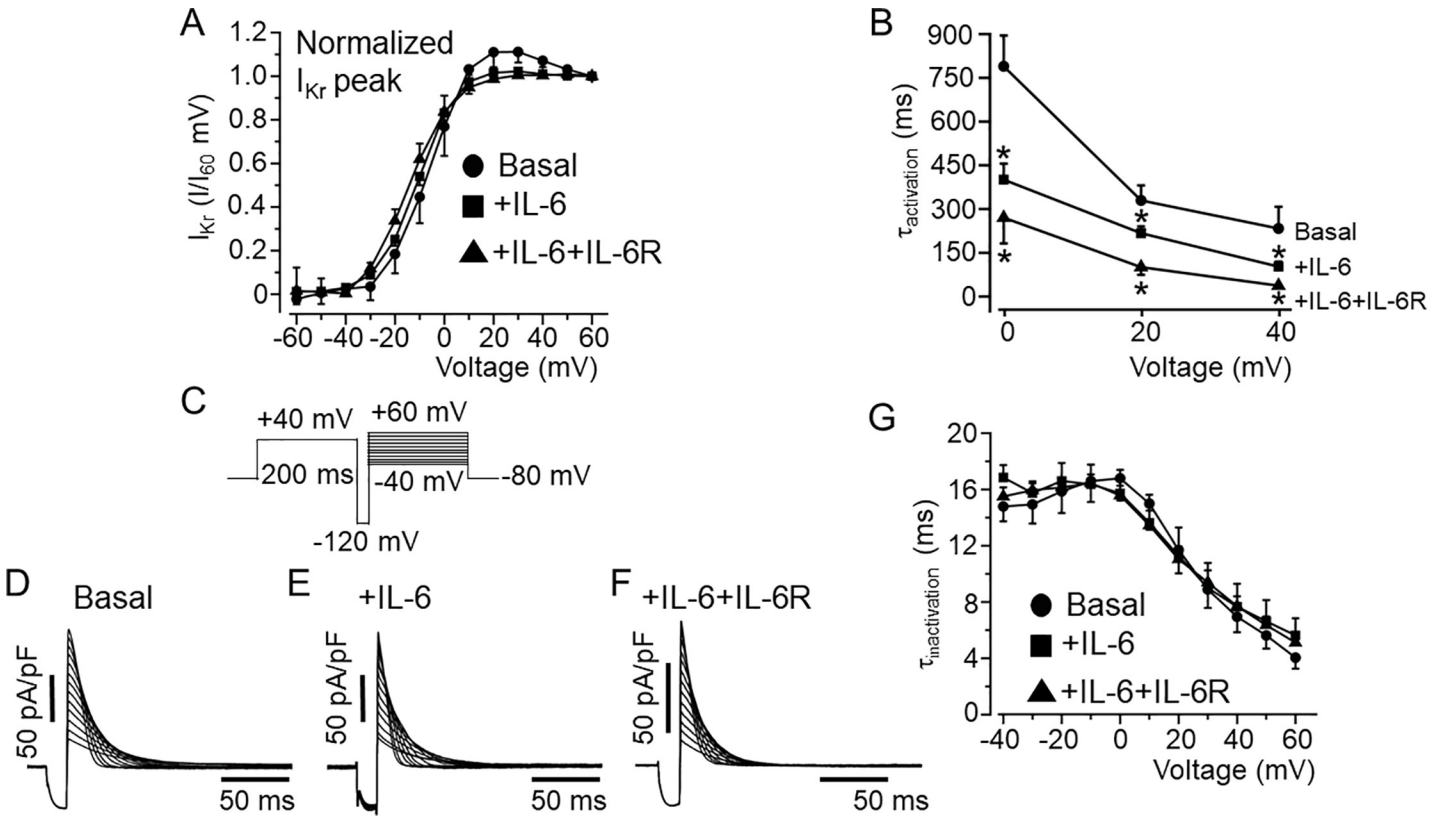

Fig 2. Effects of IL-6 on I_{Kr} activation and inactivation kinetics in HEK-hERG cells. *A*, Plots of I_{Kr} tail I/I_{+60mV} for control and in the presence of IL-6 alone and IL-6 +IL-6R. Compared to control I_{Kr} currents (circle, n = 21), the normalized tail currents show that I_{Kr} activates at more negative potentials in the presence IL-6 (square, n = 18) and IL-6+IL-6R (triangle, n = 9). *B*, Plots of activation time course ($\tau_{activation}$) and voltage relationship for basal I_{Kr} (circle, n = 21), and in the presence of IL-6 (square, n = 18) or IL-6+IL-6R (triangle, n = 9). The time course of inactivation ($\tau_{inactivation}$) was examined using the protocol shown in *C*. *D*, representative I_{Kr} current traces recorded under basal conditions, and in the presence of IL-6 (*E*) or IL-6+IL-6R (*F*). *G*, graph of the voltage-dependence of the $\tau_{inactivation}$ during basal I_{Kr} (circle, n = 8), +IL-6 (square, n = 7), +IL-6+IL-6R (triangle, n = 5) conditions.

https://doi.org/10.1371/journal.pone.0208321.g002

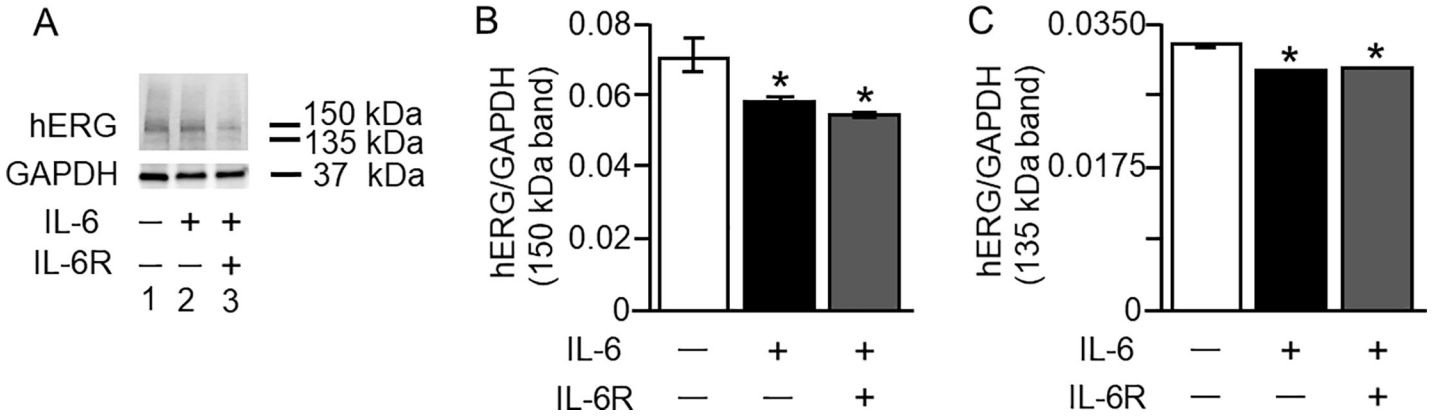

Fig 3. Effect of IL-6 on I_{Kr} protein expression in HEK-hERG cells. Western blot analysis of the I_{Kr} channel hERG expression in HEK-hERG cells from control cells and in cells pre-treated for 40 min with IL-6 (20 ng/ml) alone or IL-6 (20 ng/ml)+IL-6R (25 ng/ml). *A*, compared to control hERG protein expression (*Lane 1*), exposure to IL-6 (20 ng/ml) reduced the expression of the 150 kDa and 135 kDa (*Lane 2*) hERG proteins. A further decrease in the bands was observed (*Lane 3*) with pretreatment with IL-6 (20 ng/ml) + IL-6R (25 ng/ml). Compared to untreated HEK-hERG cells (*Open bar*, *B and C*), normalized values of 150 kDa (*B*) and 135 kDa (*C*) hERG bands/GAPDH revealed significant down-regulation of the protein expression of hERG in the presence of IL-6 alone (*Black Bars*, *B and C*) or IL-6+IL-6R (*Grey Bars*, *B and C*). Equal amounts of protein were loaded in each lane. The 37 kDa bands represent GAPDH.

https://doi.org/10.1371/journal.pone.0208321.g003

3), revealed reduced expression of the 150 kDa band. Average densitometry analysis demonstrated that IL-6 significantly reduced the 150 kDa expression by 16% (from 0.070±0.000311 to 0.059±0.000427, n = 5, *P<0.05, Fig 3B), and by 21% (from 0.070±0.0001 to 0.055±0.000427, *P<0.05) in the presence of IL-6R. Similarly, the 135 kDa band (Fig 3A) was reduced by IL-6 from 0.033±0.0001 to 0.029±0.0000424 (n = 5, Fig 3C, *P<0.05) and by IL-6+IL-6R to 0.029 ±0.000015 (n = 5, Fig 3C, *P<0.05).

IL-6 reduced I_{Kr} density through the IL-6R and JAK signaling pathways in HEK-hERG cells

The results presented in Fig 1 show that inhibition of I_{Kr} by IL-6 is more profound with IL-6R. To investigate whether IL-6 acts on I_{Kr} via IL-6R in HEK-hERG cells, we incubated IL-6R (25 ng/ml) with an inhibitory mouse monoclonal anti-IL-6R antibody (20–100 μg/ml, H-7: sc-373708, Santa Cruz, Dallas, TX, USA) for 40 minutes at room temperature. The mixture was then added to cells in combination with IL-6 (20 ng/ml) for 40 minutes before measuring I_{Kr} using the protocol shown in Fig 4A. Control I_{Kr} peak and tail currents measured in untreated HEK-hERG cells is shown in Fig 4B. In 4 separate experiments pre-treatment of cells with anti-IL-6R antibody (Fig 4C), completely prevented the inhibitory effects of IL-6 on I_{Kr}, but did not alter the currents when used alone (Data not shown). In the presence of anti-IL-6R antibody, I_{Kr} peak and tail current densities were 46.5±8.44 pA/pF (n = 4, P>0.05, Fig 4E) and 67.6±10.02 pA/pF (n = 4, P>0.05, Fig 4E) respectively, when compared to basal I_{Kr}. To investigate the involvement of Janus Kinase (JAK), we assessed I_{Kr} in the presence of IL-6+IL-6R in HEK-hERG cells pre-exposed to a JAK inhibitor-I (5 μM) [38] for 30 minutes. Pre-treatment of cells with JAK inhibitor-I also prevented the inhibitory effect of IL-6 on I_{Kr} (Fig 4D). With JAK inhibitor-I, averaged I_{Kr} peak and tail current densities were 50.05±8.81 pA/pF (n = 4, P>0.05, Fig 4E and 4F) and 65.46±11.2 pA/pF (n = 4, P>0.05, Fig 4F) respectively and similar to control I_{Kr} peak (Fig 4E) and tail (Fig 4F) densities. Normalizing peak I_{tail} curves to the maximal current at +60 mV obtained in the presence of anti-IL-6R antibody and JAK inhibitor-I revealed plots and $V_{1/2}$ values that were like control (Fig 4E). $V_{1/2}$ was -5.67±1.33 mV (n = 4, P>0.05, and -3.46±4.16 mV, n = 4, P>0.05) in the presence of anti-IL-6R antibody and JAK inhibitor-I respectively.

IL-6 inhibits I_{Kr} via Janus Kinase in freshly isolated guinea-pig ventricular cardiomyocytes

We next assessed the effect of IL-6 on native I_{Kr} from AGPVM. This was investigated by using chromanol 293B (100 μM) to block the slowly-activating delayed rectifier K current, I_{Ks} in addition to the use of a short-test depolarizing pulse protocol (200 ms, Fig 5A) during which a negligible amount of I_{Ks} will be activated, but allows a sufficient activation of a tail current upon repolarization which is largely due to slow deactivation of I_{Kr} [39]. In untreated myocytes, short depolarizing pulses evoked large outward deactivating tail currents (Fig 5B). Like the observations in HEK-hERG cells, IL-6 alone (Fig 5C) or IL-6+IL-6R (Fig 5D) significantly reduced currents at potentials positive to 10 mV. Compared to averaged control values (0.24 ±0.02 pA/pF, n = 15, Fig 5E) measured at +20 mV, I_{Kr} current densities were reduced by 45.8% (or to 0.13±0.02 pA/pF, n = 8 *P<0.05) in the presence of IL-6 alone, and by 58.3%, (0.10±0.05 pA/pF, n = 5, *P<0.05) with IL-6+IL-6R. To test whether IL-6 exerted its inhibitory effect on I_{Kr} via IL-6R and downstream JAK signaling, experiments were performed in the presence of anti-IL-6R monoclonal antibody (100 μg/ml), and JAK inhibitor-I (5 μM) respectively. Compared to control I_{Kr} (Fig 5F), pretreatment with IL-6+IL-6R+anti-IL-6R antibody (Fig 5G) or IL6+IL-6R+JAK inhibitor-I (Fig 5H) abolished the inhibitory effects of IL-6+IL-6R (Fig 5I).

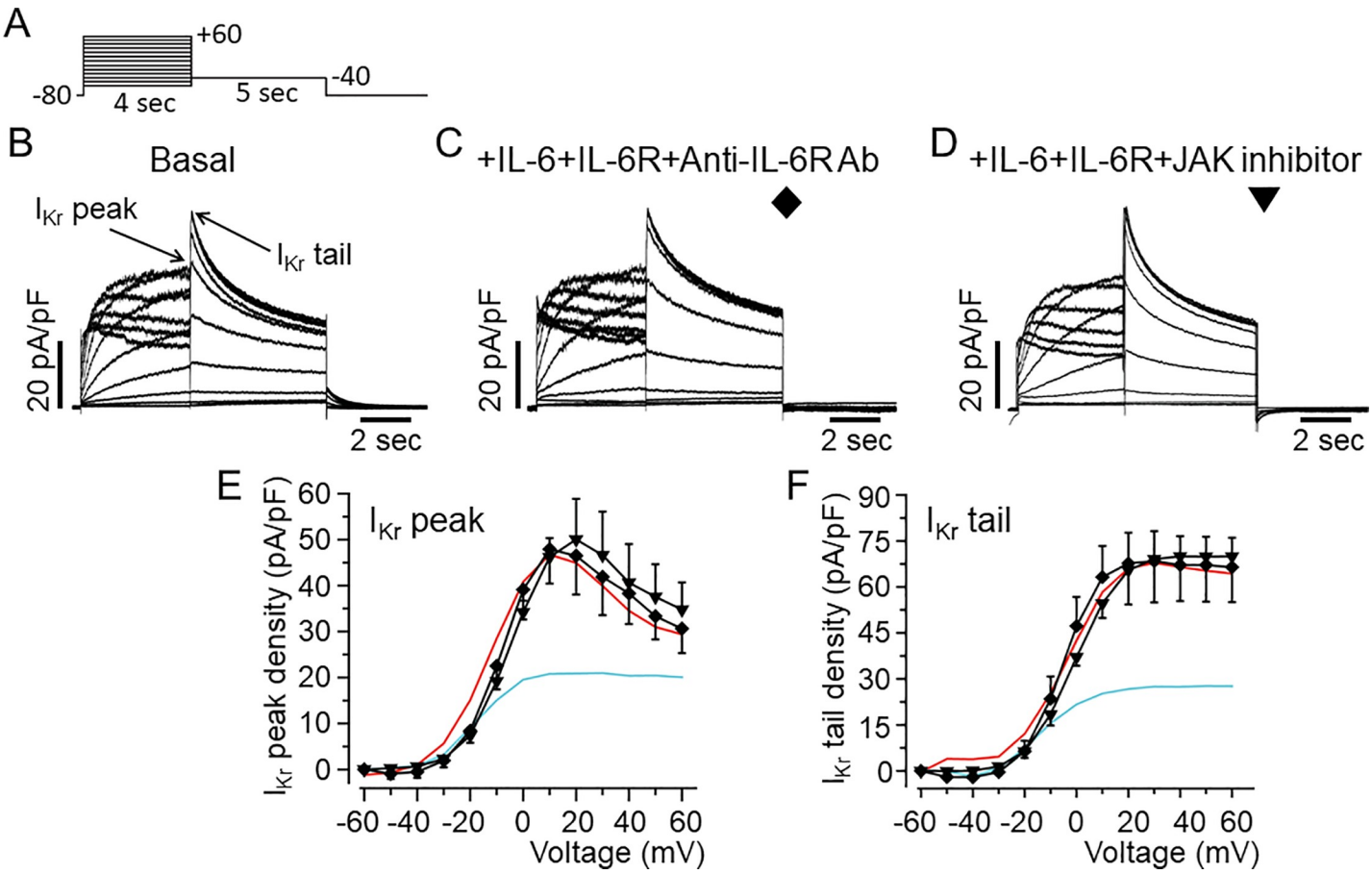

Fig 4. Inhibition of I_{Kr} by IL-6 is prevented by IL-6R and Janus Kinase blockade in HEK293 cells. *A*, Voltage-clamp protocol used to generate I_{Kr} in HEK-hERG cells stably expressing hERG channel. *B*, Basal hERG currents. *Arrows* indicate hERG peak and tail currents. *C*, Representative I_{Kr} traces from HEK-hERG cells pretreated with IL-6+IL-6R in the presence of anti-IL-6R antibody (Ab). *D*, I_{Kr} currents measured in HEK-hERG cells pre-treated with IL-6+IL-6R and the JAK inhibitor-1. Plots of I_{Kr} peak current density-voltage (*E*) and tail current density-voltage curves (*F*) in the presence of anti-IL-6R antibody (n = 4) and the JAK inhibitor-1 (n = 4). I_{Kr} peak current and tail density-voltage curves for I_{Kr} measured in basal condition (*Red line*) and in cells pre-treated with IL-6+IL-6R (*Cyan line*) are shown for comparison.

https://doi.org/10.1371/journal.pone.0208321.g004

We examined whether the endogenous IL-6Rα transcript and protein are expressed in guinea-pig heart using qRT-PCR and Western blots. Compared to control (water) (*Lane 1*), the results show that IL-6R is robustly expressed as a 120 bp band in both the atria (*Lane 2*) and ventricles (*Lane* 3, *Fig 6A*) in guinea-pig heart. Western blots of guinea pig ventricular cell lysates probed with anti-IL6Rα IL-6 antibody (H-7) further show that IL-6Rα protein expression which is manifested as an 80 kDa band (*Fig 6B*, *lane 1*) that was not seen when IL-6Rα antibody was pre-incubated with its own blocking peptide (*Fig 6B*, *lane 2*), in-line with reported data in rat heart [38].

Furthermore, IL-6 did not have any measurable effects on the densities of the inwardly rectifying *K* current (I_{K1}, *Fig 7C*) and voltage-gated Na current (I_{Na}, *7G*) at all voltages tested (*Fig 7D & 7H*) demonstrating that the inhibition of I_{Kr} by IL-6 is specific and does not indiscriminately inhibit all currents.

IL-6 regulates guinea-pig ERG expression in ventricular cardiomyocytes

To determine whether the effects of IL-6 on hERG channel expression observed in HEK-hERG cells are recapitulated in cardiomyocytes, we performed qRT-PCR and Western blot

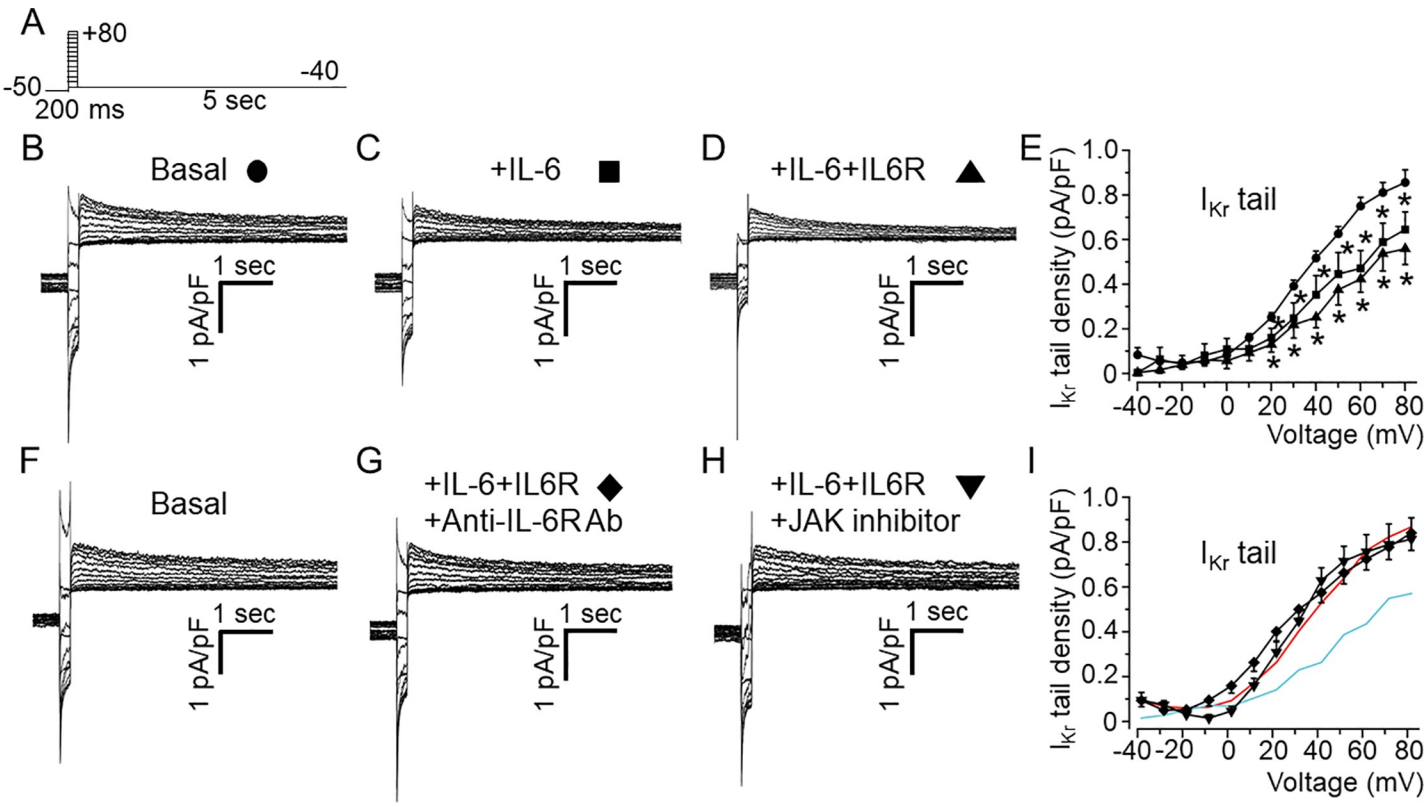

Fig 5. Effects of IL-6 and IL-6+IL-6R on I_{Kr} in adult guinea-pig ventricular myocytes. *A*, Voltage protocol used for evoking I_{Kr} in freshly isolated ventricular myocytes from adult guinea-pig heart. Tail current traces measured in the presence of 100 μM chromanol 293B and 5 μM nifedipine in control untreated cardiomyocyte (*B*, circle, n = 15), and myocytes pre-treated with IL-6 alone (*C*, square, n = 8) or IL-6 +IL-6R (*D*, upward triangle, n = 5). *E*, Population I_{Kr} tail density-voltage curves in basal, IL-6- and IL-6R-treated adult guinea-pig ventricular cardiomyocytes. *F*, Representative I_{Kr} traces in basal condition, (*G*) pre-treatment with IL-6+IL-6R in the presence of anti-IL-6R antibody (Ab) at 100 μg/ml or, *H*) a JAK inhibitor-I (5 μM). *I*, the mean I_{Kr} tail density-voltage curves show that the inhibitory effect of IL-6+IL-6R on I_{Kr} is reversed in the presence of anti-IL-6R antibody (diamond, n = 12) or JAK inhibitor I (downward triangle, n = 5). For visual comparison, data for control I_{Kr} (*Red trace*) and in the presence of IL-6+IL-6R (*Cyan trace*) in *I*.

https://doi.org/10.1371/journal.pone.0208321.g005

assays. IL-6 (20 ng/ml) significantly reduced transcript (*Fig 8A*) and protein expression of adult guinea pig ERG ventricular myocytes (*Fig 8B–8D*). Relative to control (or in the absence of IL-6), guinea pig ERG mRNA was significantly reduced by 48% (n = 3, $^{*}P<0.05$). Guinea pig ERG protein expression quantified as the 150 kDa (*Lane 1*, *Fig 8B*) band is significantly reduced by 32% (or from 0.229±0.002, n = 5, to 0.157±0.00018, n = 5, $^{*}P<0.05$), while the 135 kDa band (*Lane 2*, *Fig 8B*) is significantly reduced from 0.245±0.000447 to 0.138±0.000671 (or by 43.6%, n = 5, $^{*}P<0.05$, *Fig 8D*).

Modulation of ventricular action potential duration by IL-6/IL-6R/JAK

Finally, we examined the effect of IL-6/IL-6R on action potential duration measured in AGPVM. IL-6 significantly increased APD at 90% repolarization (APD_{90}) from 310±12.4 ms (*Black trace)*, to 371±13.9 ms (*Red trace;* 19%, n = 11, $^{*}P<0.05$, *Fig 8E and 8F*), but had a more pronounced effect in the presence of IL-6R (*Grey trace*) as APD_{90} increased to 408±27.8 ms (or by 32%, n = 14, $^{*}P<0.05$). Inhibition of JAK with JAK inhibitor-I (5 μM, *Cyan trace*) [38], or AG490 (5 μM, *Orange trace*) [40], completely prevented APD prolongation (*Fig 8E and 8F*). Compared to control APD_{90} (310±12.4 ms), values were 312.5±24.7 ms ($P>0.05$, n = 7, *Fig 8E and 8F*) and 325.5±9.43 ms (n = 6, $P>0.05$, *Fig 8E*) with JAK inhibitor and AG490 respectively.

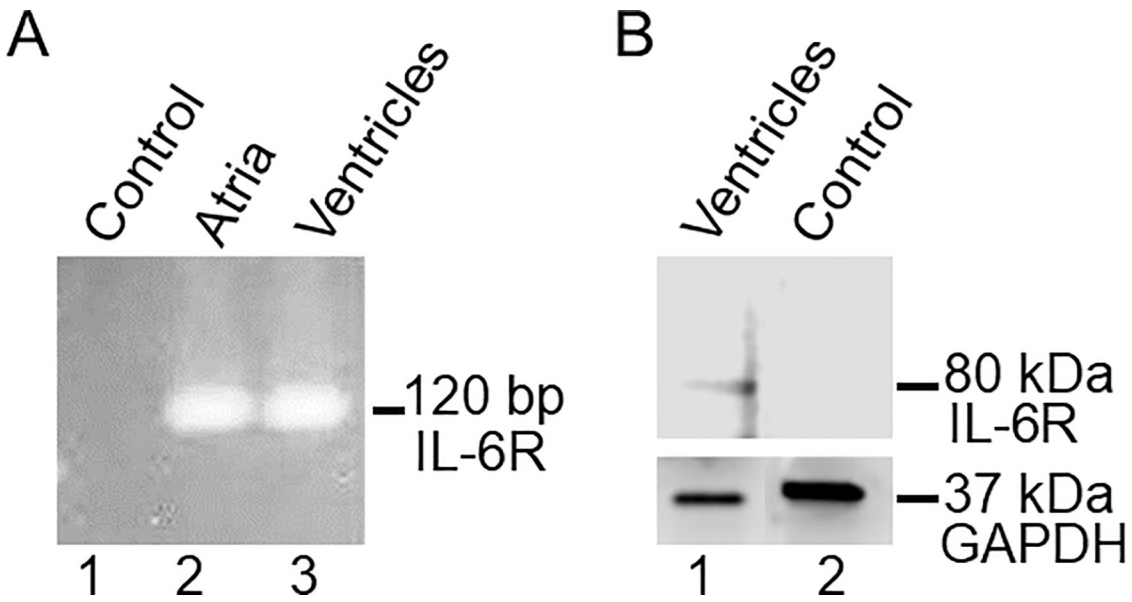

Fig 6. Transcript and protein expression of IL-6R in guinea pig heart. *A*, qRT-PCR assay for detection of IL-6R mRNA expression in guinea-pig heart. Compared to control (*Lane 1*), IL-6R (120 bp) mRNA expression was detected in both atria (*Lane 2*) and ventricles (*Lane 3*) consistent with an endogenous IL-6R expression in guinea pig heart. *B*, Western blot of IL-6R from guinea-pig ventricular cell lysates. The blot was probed with anti-IL6Rα H-7. The band around 80 kDa (*Fig 6B*, *Lane 1*) represents IL-6Rα which was absent when IL-6Rα Ab was pre-incubated with its own blocking peptide (*Fig 6B*, *Lane 2*).

https://doi.org/10.1371/journal.pone.0208321.g006

Discussion

Autoimmune inflammatory disorders are associated with an increased risk for QT_c prolongation and *TdP*, thereby contributing to the incidence of SCD [15, 22]. Here, we show that IL-6 suppresses I_{Kr} in heterologous cells and myocytes resulting in prolonged APD. Furthermore, IL-6 also markedly blunted hERG/I_{Kr} channel mRNA and protein expression. To our knowledge, there have been no previous reports on IL-6 modulation of I_{Kr} in any cell type. Thus elevated IL-6 levels, reduced I_{Kr} and associated action potential prolongation described here may contribute to delayed repolarization and associated ventricular arrhythmias such as *TdP* reported in patients with autoimmune inflammatory disorders [22].

Comparison to previous studies on cytokines and cardiac *K* channels

As pointed out above, there are no studies on the functional impact of IL-6 on hERG/*IKr* channel to date. However, and in support to this study, *Wang et al* [25] showed that another cytokine, TNF-α reduced I_{HERG} in HEK293 cells and I_{Kr} in dog ventricular myocytes. TNF-α has also been shown to reduce I_{to} in rat ventricular myocytes [26, 27]. Similarly, IL-1β inhibited I_{to} in mouse ventricular cardiomyocytes [30]. Therefore, taken together our data are consistent with the concept of modulation of cardiac *K* channels by cytokines.

We also found that inhibition of IL-6R or JAK prevented the effects of IL-6 on I_{Kr} recorded in heterologous cells and myocytes indicating that the inhibitory effect of IL-6 on I_{Kr} involves IL-6R and gp130 downstream pathways. This is in line with previous reports that JAK is a downstream pathway of IL-6 via gp130 in cardiomyocytes [41]. Other studies demonstrated that excess levels of pro-inflammatory cytokines also play a role in causing LQT, possibly through mechanisms that involve reactive oxygen species [25, 26] and ceramide signaling pathway [42, 43]. Our findings reveal a novel and/or distinct IL-6/IL-6R-JAK-I_{Kr} signaling pathway involved in acquired LQT in inflammation.

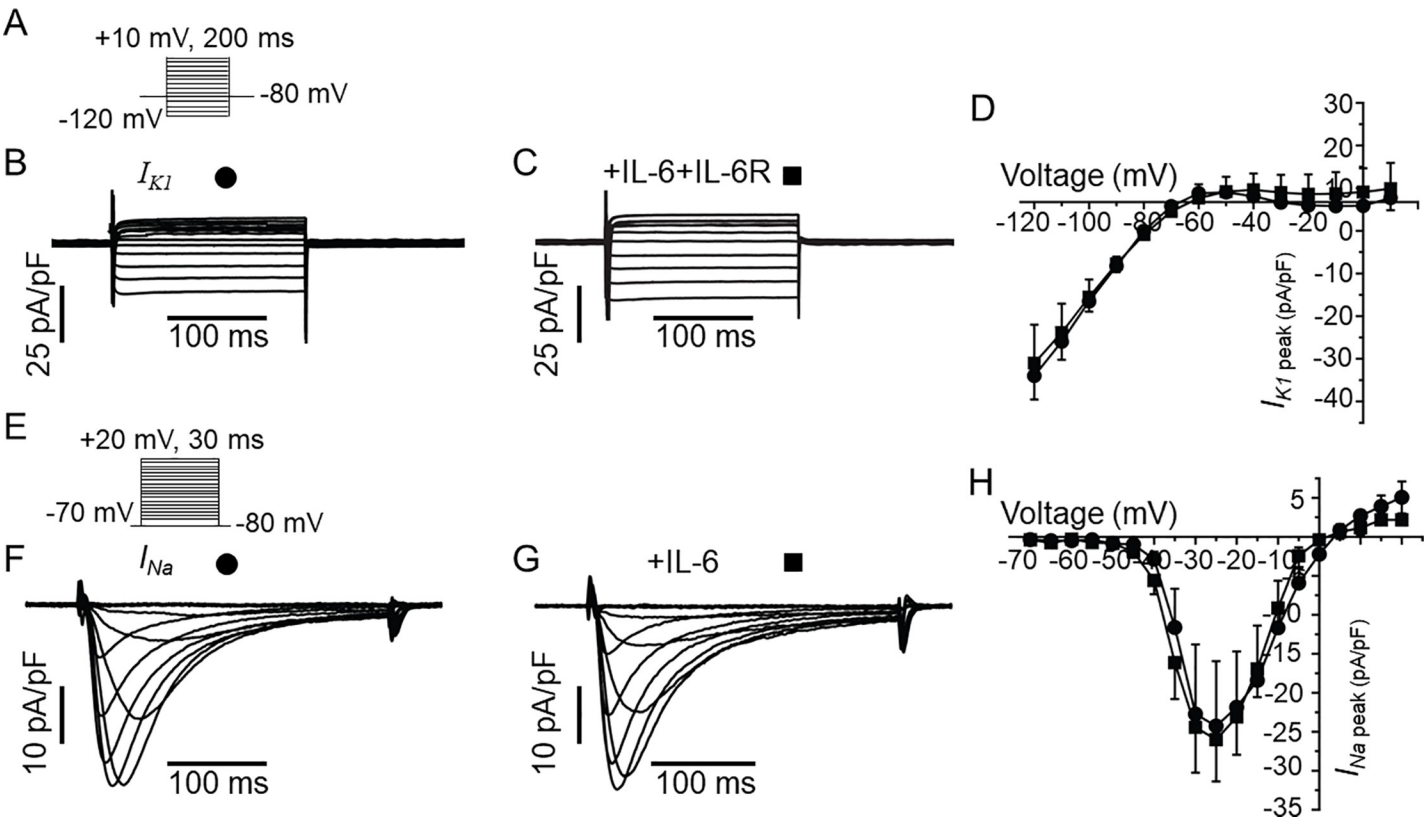

Fig 7. IL-6 has no effect on I_{K1} or I_{Na} in guinea-pig ventricular myocytes. *A*, Voltage protocol for activation of I_{K1}. Representative I_{K1} traces for a control myocyte (*B*) and from an IL-6+IL-6R pre-treated myocyte (*C*). *D*, Population I_{K1} peak density-voltage curves show that I_{K1} was not altered in IL-6-IL-6R pre-treated myocytes (square, n = 4) compared to untreated myocytes (circle, n = 3) at all voltages between -120 mV to +10 mV. *E*, The voltage protocol for evoking I_{Na}. Representative traces showing that I_{Na} measured in control cardiomyocytes (*F*) are identical to I_{Na} recorded in myocytes pre-treated with IL-6 alone (*G*). *H*, pooled data for I_{Na} peak-voltage in untreated (circle, n = 6), and IL-6-treated myocytes (square, n = 6).

https://doi.org/10.1371/journal.pone.0208321.g007

There have also been reports of cytokine's effects on cardiac *K* channel subunit gene and protein expression with contradicting results. While Petkova-Kirova *et al* [29] and Fernandez-Velasco *et al* [26] reported reduced cardiac *K* channels protein expression with TNF-α, Grandy & Fiset [44] reported no changes. In this study, IL-6 decreased expression of hERG proteins which occurred within 40 minutes suggesting that IL-6 alone or in combination with IL-6R may depress hERG expression by accelerating the channel turnover at multiple levels including at the transcriptional, translational as well as channel turnover at the cell-surface. Furthermore, in addition to significant inhibition in I_{Kr} current, we find that IL-6 pre-treated HEK-hERG cells displayed reduced I_{Tails}, a leftward shift in $V_{1/2}$ of activation, and time-course of activation both of which were further pronounced in the presence of IL-6R. These mechanistic insights are likely to have important implications for predicting the functional impact of temporal changes in cytokine levels, functional expression of *K* channels, and cardiac repolarization. Therefore, the inhibitory effect of IL-6 on I_{Kr} can be attributed, at least in part, to both channel gating and protein trafficking.

Previous studies have also shown reduced outward *K* currents and a prolonged APD in isolated myocytes incubated with TNF-α [25, 26] or IL-1β [30]. In contrast, Grandi and Fiset [44] showed that ventricular APD was not altered in TNF-α treated mice, despite reduced I_{to} and I_{Kur}. Recently George *et al* [45] also demonstrated lack of a prolonged APD with TNF-α in atrial myocytes isolated from adult guinea-pigs although voltage-gated *K* currents were not

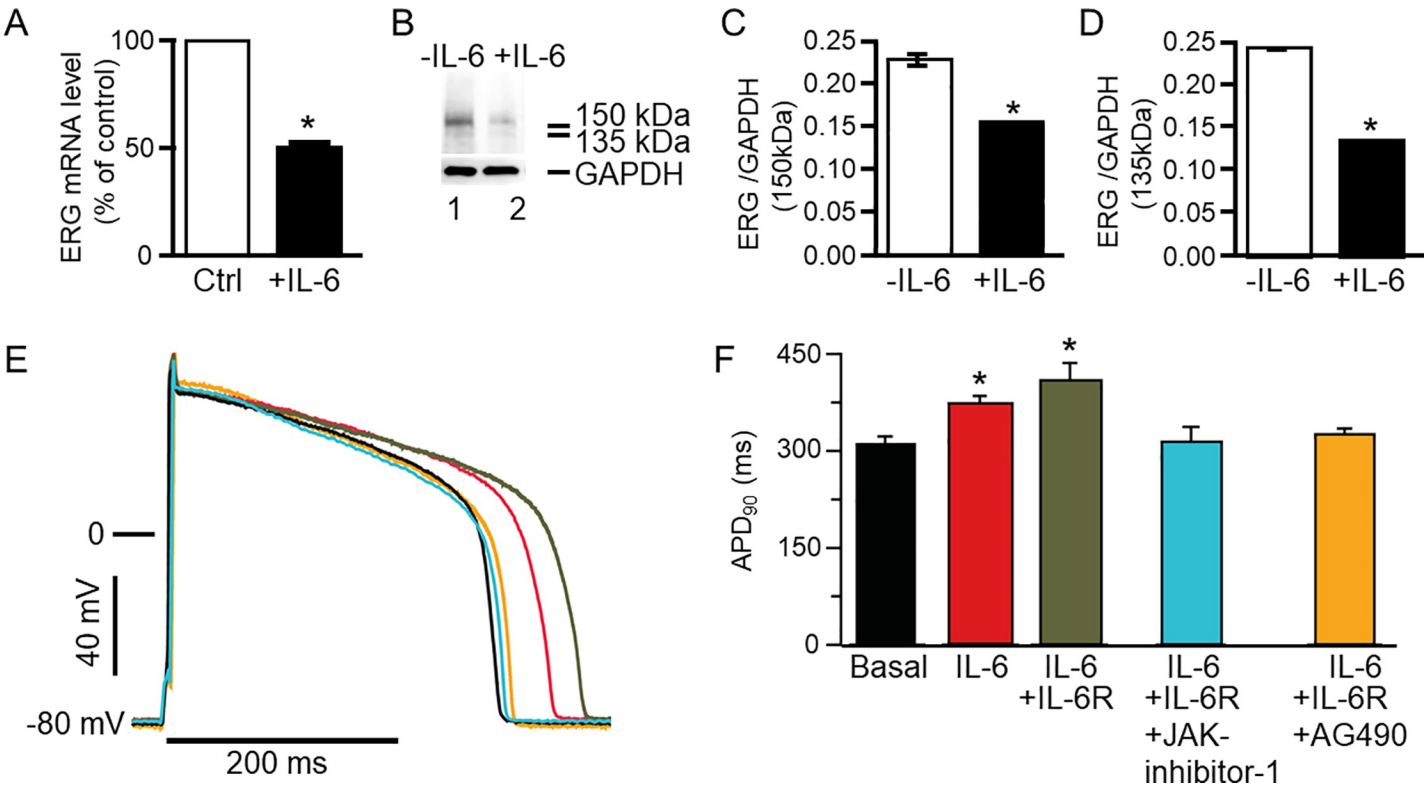

Fig 8. Effect of IL-6 on *guinea pig ERG* expression and action potential in ventricular myocytes. *A*, qRT-PCR was used to determine guinea pig ether-á-go-go-related gene (ERG) mRNA expression in control ventricular myocytes and in myocytes pre-treated with IL-6 (20 ng/ml). *B*, Western blot assay of guinea pig ERG protein expression in control (*Lane 1*) and IL-6 pretreated (for 40 mins) myocytes (*Lane 2*). Values were normalized to the GAPDH signal and expressed as % of control or in the absence of IL-6. Each sample was analyzed in triplicate. 150 kDa and 135 kDa ERG bands were identified in lane 1 but were significantly less dense in lane 2 loaded with IL-6 (20 ng/ml) pretreated ventricular myocytes' lysate. *C*, Comparison of the relative abundance of the 150 kDa ERG band in untreated and IL-6 treated myocytes. *D*, Comparison of the relative abundance of the 135 kDa ERG band in untreated and IL-treated myocytes. The 37 kDa bands represent GAPDH. *E*, Action potential waveforms recorded in control myocytes (basal conditions without IL-6, *Black trace*) and in the presence of IL-6 alone (*Red trace*), IL-6+IL-6R (*Grey trace*), IL-6+IL-6R +JAK inhibitor-1 (*Cyan trace*) and another JAK inhibitor AG490 (*Orange trace*). *F*, Pretreatment of myocytes with IL-6 and IL-6+IL-6R significantly prolonged APD_{90} and JAK inhibitor I and AG490 completely reversed the prolongation of the action potential.

https://doi.org/10.1371/journal.pone.0208321.g008

measured in these studies. However, APD prolongation and heart failure were reported by London *et al* [46] in transgenic mice overexpressing TNF-α and by Wang *et al* [25] in dog ventricular myocytes. Therefore, one can speculate that our findings suggest that IL-6 may also be an important contributor to I_{Kr} reduction in heart failure [47].

Finally, IL-6 is emerging as one of the relevant cytokines involved in the inflammatory process with cardiac electrophysiological consequences [5]. The physiological relevance of this study is underscored by focusing specifically on the individual effects of IL-6 on I_{Kr} channel function. This is an important step prior to identifying whether common mechanisms underlie the complex electrical remodeling process associated with the cumulative effects of inflammatory factors that occur during the complex process of cardiac and systemic inflammation that predispose to arrhythmic events. IL-6 inhibition has also been developed as a therapy for diseases associated with inflammation [48]. These efforts are likely to increase our understanding of how IL-6 and its inhibitors may affect cardiac electrical function. In this regard, the IL-6R inhibitor tocilizumab [49], which is widely used clinically to treat RA [50], may also have an emerging role as an anti-arrhythmic drug [9, 51].

Conclusion

Overall, the present study is first to demonstrate that pathologically elevated IL-6 levels can negatively modulate I_{Kr}. Our findings are consistent with the notion that changes in IL-6 in individuals with systemic inflammation related to autoimmune disorders (but also possibly to infections or other inflammatory diseases) may display blunted I_{Kr} with serious implications for cardiac repolarization especially in the setting of other known classical risk factors including electrolytes imbalance, QT_c prolonging medications, genetic and autoimmune channelopathies [22]. Our results predict specific inhibitors of IL-6R or cellular mediators that enhance channel opening to normalize I_{Kr} would be expected to correct QT_c prolongation in patients. By providing the first measurements of the effect of IL-6 on hERG/I_{Kr}, we reveal that I_{Kr} is sensitive to pathological changes in cytokine levels in cardiac and systemic inflammation. Collectively our findings open new directions in determining the contribution of other downstream complex effectors (STAT3, MAPK, Pi3K/Akt) in IL-6-associated signaling pathways on I_{Kr}. This study was undertaken in both native guinea-pig ventricular myocytes and HEK293 cells stably expressing hERG/$I_{Kr,}$ both of which exhibited similar findings. It will be interesting to confirm these outcomes in other system models such as human induced pluripotent cells-derived cardiomyocytes or in vivo animal models. Regardless, the data clearly show that IL-6 depresses I_{Kr} through IL-6R and JAK pathways, suggesting a novel cytokine mechanism in acquired inflammation induced LQTS.

Clinical perspectives

wPro-inflammatory IL-6 cytokine-mediated changes in cardiomyocyte ion channel function is a novel risk factor involved in the acquired inflammatory LQTS, a condition that underlies impaired repolarization, leading to ventricular arrhythmias and SCD. The translational implications are that patients with inflammatory disorders with high levels of IL-6 can benefit from routine ECG and counselling if other QT_c prolonging risk factors are present in these patients.

Acknowledgments

This work was supported by the American Heart Association (13SDG16850065 to A.S.A.); and a Merit Review grant I01 BX002137 from Biomedical Laboratory Research & Development Service of Veterans Affairs Office of Research and Development (to M.B).

Author Contributions

Conceptualization: Pier Leopoldo Capecchi, Franco Laghi-Pasini, Pietro Enea Lazzerini, Mohamed Boutjdir.

Data curation: Ademuyiwa S. Aromolaran, Ujala Srivastava.

Funding acquisition: Ademuyiwa S. Aromolaran, Mohamed Boutjdir.

Methodology: Alessandra Alí.

Writing – original draft: Ademuyiwa S. Aromolaran.

Writing – review & editing: Ademuyiwa S. Aromolaran, Mohamed Chahine, Deana Lazaro, Nabil El-Sherif, Pier Leopoldo Capecchi, Franco Laghi-Pasini, Pietro Enea Lazzerini, Mohamed Boutjdir.

References

1. Yang S, Zheng R, Hu S, Ma Y, Choudhry MA, Messina JL, et al. Mechanism of cardiac depression after trauma-hemorrhage: increased cardiomyocyte IL-6 and effect of sex steroids on IL-6 regulation and cardiac function. American journal of physiology Heart and circulatory physiology. 2004; 287(5):H2183–91. Epub 2004/10/12. https://doi.org/10.1152/ajpheart.00624.2003 PMID: 15475534.
2. Fontes JA, Rose NR, Cihakova D. The varying faces of IL-6: From cardiac protection to cardiac failure. Cytokine. 2015; 74(1):62–8. Epub 2015/02/05. https://doi.org/10.1016/j.cyto.2014.12.024 PMID: 25649043; PubMed Central PMCID: PMCPmc4677779.
3. Naka T, Nishimoto N, Kishimoto T. The paradigm of IL-6: from basic science to medicine. Arthritis Res. 2002; 4 Suppl 3:S233–42. Epub 2002/07/12. https://doi.org/10.1186/ar565 PMID: 12110143; PubMed Central PMCID: PMCPMC3240141.
4. Kurdi M, Booz GW. Can the protective actions of JAK-STAT in the heart be exploited therapeutically? Parsing the regulation of interleukin-6-type cytokine signaling. J Cardiovasc Pharmacol. 2007; 50 (2):126–41. Epub 2007/08/19. https://doi.org/10.1097/FJC.0b013e318068dd49 PMID: 17703129.
5. Lazzerini PE, Laghi-Pasini F, Bertolozzi I, Morozzi G, Lorenzini S, Simpatico A, et al. Systemic inflammation as a novel QT-prolonging risk factor in patients with torsades de pointes. Heart (British Cardiac Society). 2017. Epub 2017/05/12. https://doi.org/10.1136/heartjnl-2016-311079 PMID: 28490617.
6. Adlan AM, Panoulas VF, Smith JP, Fisher JP, Kitas GD. Association between corrected QT interval and inflammatory cytokines in rheumatoid arthritis. The Journal of rheumatology. 2015; 42(3):421–8. Epub 2015/01/17. https://doi.org/10.3899/jrheum.140861 PMID: 25593223.
7. Lazzerini PE, Capecchi PL, Laghi-Pasini F. Long QT Syndrome: An Emerging Role for Inflammation and Immunity. Frontiers in cardiovascular medicine. 2015; 2:26. Epub 2016/01/23. https://doi.org/10.3389/fcvm.2015.00026 PMID: 26798623; PubMed Central PMCID: PMCPmc4712633.
8. Ukena C, Mahfoud F, Kindermann I, Kandolf R, Kindermann M, Bohm M. Prognostic electrocardiographic parameters in patients with suspected myocarditis. European journal of heart failure. 2011; 13(4):398–405. Epub 2011/01/18. https://doi.org/10.1093/eurjhf/hfq229 PMID: 21239404.
9. Lazzerini PE, Acampa M, Capecchi PL, Fineschi I, Selvi E, Moscadelli V, et al. Antiarrhythmic potential of anticytokine therapy in rheumatoid arthritis: tocilizumab reduces corrected QT interval by controlling systemic inflammation. Arthritis care & research. 2015; 67(3):332–9. Epub 2014/09/05. https://doi.org/10.1002/acr.22455 PMID: 25186226.
10. Medenwald D, Kors JA, Loppnow H, Thiery J, Kluttig A, Nuding S, et al. Inflammation and prolonged QT time: results from the Cardiovascular Disease, Living and Ageing in Halle (CARLA) study. PloS one. 2014; 9(4):e95994. Epub 2014/04/29. https://doi.org/10.1371/journal.pone.0095994 PMID: 24770373; PubMed Central PMCID: PMCPmc4000193.
11. Pujades-Rodriguez M, Duyx B, Thomas SL, Stogiannis D, Rahman A, Smeeth L, et al. Rheumatoid Arthritis and Incidence of Twelve Initial Presentations of Cardiovascular Disease: A Population Record-Linkage Cohort Study in England. PloS one. 2016; 11(3):e0151245. Epub 2016/03/16. https://doi.org/10.1371/journal.pone.0151245 PMID: 26978266; PubMed Central PMCID: PMCPmc4792375.
12. Maradit-Kremers H, Crowson CS, Nicola PJ, Ballman KV, Roger VL, Jacobsen SJ, et al. Increased unrecognized coronary heart disease and sudden deaths in rheumatoid arthritis: a population-based cohort study. Arthritis Rheum. 2005; 52(2):402–11. Epub 2005/02/05. https://doi.org/10.1002/art.20853 PMID: 15693010.
13. Lazzerini PE, Acampa M, Capecchi PL, Hammoud M, Maffei S, Bisogno S, et al. Association between high sensitivity C-reactive protein, heart rate variability and corrected QT interval in patients with chronic inflammatory arthritis. European journal of internal medicine. 2013; 24(4):368–74. Epub 2013/03/23. https://doi.org/10.1016/j.ejim.2013.02.009 PMID: 23517852.
14. Chauhan K, Ackerman MJ, Crowson CS, Matteson EL, Gabriel SE. Population-based study of QT interval prolongation in patients with rheumatoid arthritis. Clinical and experimental rheumatology. 2015; 33 (1):84–9. Epub 2015/01/13. PMID: 25572282; PubMed Central PMCID: PMCPmc4366055.
15. Lazzerini PE, Capecchi PL, Laghi-Pasini F. Systemic inflammation and arrhythmic risk: lessons from rheumatoid arthritis. European heart journal. 2017; 38(22):1717–27. Epub 2016/06/03. https://doi.org/10.1093/eurheartj/ehw208 PMID: 27252448.
16. Lazzerini PE, Capecchi PL, Acampa M, Galeazzi M, Laghi-Pasini F. Arrhythmic risk in rheumatoid arthritis: the driving role of systemic inflammation. Autoimmunity reviews. 2014; 13(9):936–44. Epub 2014/05/31. https://doi.org/10.1016/j.autrev.2014.05.007 PMID: 24874445.
17. Panoulas VF, Toms TE, Douglas KM, Sandoo A, Metsios GS, Stavropoulos-Kalinoglou A, et al. Prolonged QTc interval predicts all-cause mortality in patients with rheumatoid arthritis: an association driven by high inflammatory burden. Rheumatology (Oxford). 2014; 53(1):131–7. Epub 2013/10/08. https://doi.org/10.1093/rheumatology/ket338 PMID: 24097136.

18. Mackey RH, Kuller LH, Deane KD, Walitt BT, Chang YF, Holers VM, et al. Rheumatoid Arthritis, Anti-Cyclic Citrullinated Peptide Positivity, and Cardiovascular Disease Risk in the Women's Health Initiative. Arthritis & rheumatology (Hoboken, NJ). 2015; 67(9):2311–22. Epub 2015/05/20. https://doi.org/10.1002/art.39198 PMID: 25988241; PubMed Central PMCID: PMCPmc4551571.

19. Pisoni CN, Reina S, Arakaki D, Eimon A, Carrizo C, Borda E. Elevated IL-1beta levels in anti-Ro/SSA connective tissue diseases patients with prolonged corrected QTc interval. Clinical and experimental rheumatology. 2015; 33(5):715–20. Epub 2015/09/01. PMID: 26314292.

20. Puckerin A, Aromolaran KA, Chang DD, Zukin RS, Colecraft HM, Boutjdir M, et al. hERG 1a LQT2 C-terminus truncation mutants display hERG 1b-dependent dominant negative mechanisms. Heart Rhythm. 2016; 13(5):1121–30. https://doi.org/10.1016/j.hrthm.2016.01.012 PMID: 26775140.

21. Tristani-Firouzi M, Chen J, Mitcheson JS, Sanguinetti MC. Molecular biology of K(+) channels and their role in cardiac arrhythmias. Am J Med. 2001; 110(1):50–9. Epub 2001/01/12. PMID: 11152866.

22. Lazzerini PE, Capecchi PL, Laghi-Pasini F, Boutjdir M. Autoimmune channelopathies as a novel mechanism in cardiac arrhythmias. Nature reviews Cardiology. 2017. Epub 2017/05/05. https://doi.org/10.1038/nrcardio.2017.61 PMID: 28470179.

23. El-Sherif N, Boutjdir M. Role of pharmacotherapy in cardiac ion channelopathies. Pharmacol Ther. 2015; 155:132–42. https://doi.org/10.1016/j.pharmthera.2015.09.002 PMID: 26376080.

24. Schwartz PJ, Ackerman MJ. The long QT syndrome: a transatlantic clinical approach to diagnosis and therapy. European heart journal. 2013; 34(40):3109–16. https://doi.org/10.1093/eurheartj/eht089 PMID: 23509228.

25. Wang J, Wang H, Zhang Y, Gao H, Nattel S, Wang Z. Impairment of HERG K(+) channel function by tumor necrosis factor-alpha: role of reactive oxygen species as a mediator. The Journal of biological chemistry. 2004; 279(14):13289–92. Epub 2004/02/20. https://doi.org/10.1074/jbc.C400025200 PMID: 14973143.

26. Fernandez-Velasco M, Ruiz-Hurtado G, Hurtado O, Moro MA, Delgado C. TNF-alpha downregulates transient outward potassium current in rat ventricular myocytes through iNOS overexpression and oxidant species generation. American journal of physiology Heart and circulatory physiology. 2007; 293 (1):H238–45. Epub 2007/03/06. https://doi.org/10.1152/ajpheart.01122.2006 PMID: 17337591.

27. Kawada H, Niwano S, Niwano H, Yumoto Y, Wakisaka Y, Yuge M, et al. Tumor necrosis factor-alpha downregulates the voltage gated outward K+ current in cultured neonatal rat cardiomyocytes: a possible cause of electrical remodeling in diseased hearts. Circulation journal: official journal of the Japanese Circulation Society. 2006; 70(5):605–9. Epub 2006/04/26. PMID: 16636498.

28. Li YH, Rozanski GJ. Effects of human recombinant interleukin-1 on electrical properties of guinea pig ventricular cells. Cardiovascular research. 1993; 27(3):525–30. Epub 1993/03/01. PMID: 8490954.

29. Petkova-Kirova PS, Gursoy E, Mehdi H, McTiernan CF, London B, Salama G. Electrical remodeling of cardiac myocytes from mice with heart failure due to the overexpression of tumor necrosis factor-alpha. American journal of physiology Heart and circulatory physiology. 2006; 290(5):H2098–107. Epub 2005/12/13. https://doi.org/10.1152/ajpheart.00097.2005 PMID: 16339842.

30. Monnerat G, Alarcon ML, Vasconcellos LR, Hochman-Mendez C, Brasil G, Bassani RA, et al. Macrophage-dependent IL-1beta production induces cardiac arrhythmias in diabetic mice. Nature communications. 2016; 7:13344. Epub 2016/11/25. https://doi.org/10.1038/ncomms13344 PMID: 27882934; PubMed Central PMCID: PMCPmc5123037.

31. Hagiwara Y, Miyoshi S, Fukuda K, Nishiyama N, Ikegami Y, Tanimoto K, et al. SHP2-mediated signaling cascade through gp130 is essential for LIF-dependent I CaL, [Ca2+]i transient, and APD increase in cardiomyocytes. J Mol Cell Cardiol. 2007; 43(6):710–6. https://doi.org/10.1016/j.yjmcc.2007.09.004 PMID: 17961593.

32. Aromolaran AS, Subramanyam P, Chang DD, Kobertz WR, Colecraft HM. LQT1 mutations in KCNQ1 C-terminus assembly domain suppress IKs using different mechanisms. Cardiovascular research. 2014; 104(3):501–11. Epub 2014/10/26. https://doi.org/10.1093/cvr/cvu231 cvu231 [pii]. PMID: 25344363; PubMed Central PMCID: PMC4296111.

33. Yue Y, Castrichini M, Srivastava U, Fabris F, Shah K, Li Z, et al. Pathogenesis of the Novel Autoimmune-Associated Long-QT Syndrome. Circulation. 2015; 132(4):230–40. https://doi.org/10.1161/CIRCULATIONAHA.115.009800 PMID: 25995318.

34. Aromolaran AS, Colecraft HM, Boutjdir M. High-fat diet-dependent modulation of the delayed rectifier K (+) current in adult guinea pig atrial myocytes. Biochem Biophys Res Commun. 2016; 474(3):554–9. https://doi.org/10.1016/j.bbrc.2016.04.113 PMID: 27130822.

35. Larsen AP, Olesen SP, Grunnet M, Jespersen T. Characterization of hERG1a and hERG1b potassium channels-a possible role for hERG1b in the I (Kr) current. Pflugers Archiv: European journal of physiology. 2008; 456(6):1137–48. https://doi.org/10.1007/s00424-008-0476-7 PMID: 18504605.

36. Chen WH, Wang WY, Zhang J, Yang D, Wang YP. State-dependent blockade of human ether-a-go-go-related gene (hERG) K(+) channels by changrolin in stably transfected HEK293 cells. Acta pharmacologica Sinica. 2010; 31(8):915–22. Epub 2010/08/06. https://doi.org/10.1038/aps.2010.84 PMID: 20686516; PubMed Central PMCID: PMCPMC4007811.

37. Gustina AS, Trudeau MC. hERG potassium channel gating is mediated by N- and C-terminal region interactions. The Journal of general physiology. 2011; 137(3):315–25. https://doi.org/10.1085/jgp.201010582 PMID: 21357734; PubMed Central PMCID: PMC3047612.

38. Szabo-Fresnais N, Lefebvre F, Germain A, Fischmeister R, Pomerance M. A new regulation of IL-6 production in adult cardiomyocytes by beta-adrenergic and IL-1 beta receptors and induction of cellular hypertrophy by IL-6 trans-signalling. Cell Signal. 2010; 22(7):1143–52. https://doi.org/10.1016/j.cellsig.2010.03.009 PMID: 20227492.

39. Karle CA, Zitron E, Zhang W, Kathofer S, Schoels W, Kiehn J. Rapid component I(Kr) of the guinea-pig cardiac delayed rectifier K(+) current is inhibited by beta(1)-adrenoreceptor activation, via cAMP/protein kinase A-dependent pathways. Cardiovascular research. 2002; 53(2):355–62. Epub 2002/02/06. S0008636301005090 [pii]. PMID: 11827686.

40. Wang Y, Wang D, Zhang L, Ye F, Li M, Wen K. Role of JAK-STAT pathway in reducing cardiomyocytes hypoxia/reoxygenation injury induced by S1P postconditioning. European journal of pharmacology. 2016; 784:129–36. Epub 2016/05/25. https://doi.org/10.1016/j.ejphar.2016.05.024 PMID: 27215146.

41. Pan J, Fukuda K, Saito M, Matsuzaki J, Kodama H, Sano M, et al. Mechanical stretch activates the JAK/STAT pathway in rat cardiomyocytes. Circ Res. 1999; 84(10):1127–36. PMID: 10347087.

42. Bai X, Zhi X, Zhang Q, Liang F, Chen W, Liang C, et al. Inhibition of protein phosphatase 2A sensitizes pancreatic cancer to chemotherapy by increasing drug perfusion via HIF-1alpha-VEGF mediated angiogenesis. Cancer letters. 2014; 355(2):281–7. Epub 2014/10/12. https://doi.org/10.1016/j.canlet.2014.09.048 PMID: 25304380.

43. Sordillo PP, Sordillo DC, Helson L. Review: The Prolonged QT Interval: Role of Pro-inflammatory Cytokines, Reactive Oxygen Species and the Ceramide and Sphingosine-1 Phosphate Pathways. In vivo (Athens, Greece). 2015; 29(6):619–36. Epub 2015/11/08. PMID: 26546519.

44. Grandy SA, Fiset C. Ventricular K+ currents are reduced in mice with elevated levels of serum TNFalpha. J Mol Cell Cardiol. 2009; 47(2):238–46. Epub 2009/03/14. https://doi.org/10.1016/j.yjmcc.2009.02.025 PMID: 19281815.

45. George SA, Calhoun PJ, Gourdie RG, Smyth JW, Poelzing S. TNFalpha Modulates Cardiac Conduction by Altering Electrical Coupling between Myocytes. Frontiers in physiology. 2017; 8:334. Epub 2017/06/08. https://doi.org/10.3389/fphys.2017.00334 PMID: 28588504; PubMed Central PMCID: PMCPMC5440594.

46. London B, Baker LC, Lee JS, Shusterman V, Choi BR, Kubota T, et al. Calcium-dependent arrhythmias in transgenic mice with heart failure. American journal of physiology Heart and circulatory physiology. 2003; 284(2):H431–41. Epub 2002/10/22. https://doi.org/10.1152/ajpheart.00431.2002 PMID: 12388316.

47. Wollert KC, Drexler H. The role of interleukin-6 in the failing heart. Heart failure reviews. 2001; 6(2):95–103. Epub 2001/04/20. PMID: 11309528.

48. Narazaki M, Tanaka T, Kishimoto T. The role and therapeutic targeting of IL-6 in rheumatoid arthritis. Expert review of clinical immunology. 2017; 13(6):535–51. Epub 2017/05/12. https://doi.org/10.1080/1744666X.2017.1295850 PMID: 28494214.

49. Kikuchi J, Kondo T, Shibata A, Sakai R, Okada Y, Chino K, et al. Efficacy and tolerability of six-week extended dosing interval with tocilizumab therapy in a prospective cohort as remission maintenance in patients with rheumatoid arthritis. Modern rheumatology. 2017:1–8. Epub 2017/08/30. https://doi.org/10.1080/14397595.2017.1366092 PMID: 28849709.

50. Hashizume M, Tan SL, Takano J, Ohsawa K, Hasada I, Hanasaki A, et al. Tocilizumab, a humanized anti-IL-6R antibody, as an emerging therapeutic option for rheumatoid arthritis: molecular and cellular mechanistic insights. International reviews of immunology. 2015; 34(3):265–79. Epub 2014/08/08. https://doi.org/10.3109/08830185.2014.938325 PMID: 25099958.

51. Kleveland O, Kunszt G, Bratlie M, Ueland T, Broch K, Holte E, et al. Effect of a single dose of the interleukin-6 receptor antagonist tocilizumab on inflammation and troponin T release in patients with non-ST-elevation myocardial infarction: a double-blind, randomized, placebo-controlled phase 2 trial. European heart journal. 2016; 37(30):2406–13. Epub 2016/05/11. https://doi.org/10.1093/eurheartj/ehw171 PMID: 27161611.